

Article

Real-Time Optimal Chiller Capacity Control Based on COP Margins

Tung-Sheng Zhan ¹, Kai-Wen Chang ² and Ming-Tang Tsai ^{2,*}

¹ Department of Electrical Engineering, National Kaohsiung University of Science and Technology, Kaohsiung 807618, Taiwan; tszhan1109@nkust.edu.tw

² Department of Electrical Engineering, Cheng-Shiu University, Kaohsiung 833, Taiwan; kaimom40@yahoo.com.tw

* Correspondence: k0217@gcloud.csu.edu.tw; Tel.: +886-7-7310606

Abstract

This study proposes a real-time chiller capacity control strategy based on marginal Coefficient of Performance (COP) analysis to improve the energy efficiency of air-conditioning systems. The research focuses on the air-conditioning system (ACS) of an office building. Operational data, including chiller capacity and the corresponding COP, were collected to derive the chiller's operating characteristic curve. The Optimal Capacity Control (OCC) strategy aims to maximize the total COP of all chillers, and the initial capacity allocation is determined using the Lagrange multiplier method. To further refine performance, a fine-tuning mechanism is introduced, calculating the ratio of COP variation to capacity variation (RC ratio) for each chiller to identify which unit should be loaded or unloaded. Based on the fine-tuning mechanism, a comprehensive OCC model is established to ensure that the chiller's cooling output precisely matches the load demand, thereby maximizing system efficiency and reducing energy consumption. To validate the effectiveness of the proposed OCC strategy, a numerical analysis was implemented using real operational data from the existing ACS. Comparative simulations between the OCC and a Traditional Capacity Control (TCC) strategy were conducted. On a representative summer day, total power consumption decreased from 1534.0 kWh (TCC) to 1527.2 kWh (OCC), while total system COP increased from 113.9 to 114.8. Seasonal analysis further confirms consistent energy savings under varying load conditions. The results indicate that the OCC strategy significantly enhances system performance and reduces energy consumption under varying load conditions. Overall, the proposed method achieves a higher system COP, leading to notable electricity savings and improved operational efficiency of the air-conditioning system.

Keywords: air-conditioning system; Optimal Capacity Control (OCC); Coefficient of Performance (COP); energy efficiency



Academic Editor: Mahmoud Bourouis

Received: 3 February 2026

Revised: 25 February 2026

Accepted: 1 March 2026

Published: 3 March 2026

Copyright: © 2026 by the authors.

Licensee MDPI, Basel, Switzerland.

This article is an open access article distributed under the terms and conditions of the [Creative Commons Attribution \(CC BY\) license](https://creativecommons.org/licenses/by/4.0/).

1. Introduction

In Taiwan, air-conditioning systems have become indispensable to daily life, accounting for more than 40% of the total electricity consumption. Consequently, their share of overall power demand has been steadily increasing, particularly due to the rapid proliferation of small- and medium-sized air-conditioning systems (ACS), which has driven peak electricity loads to new record levels. Furthermore, climate change induced by the greenhouse effect is projected to raise the average temperature on peak demand days in

Taiwan. For most users, ACS is primarily operated during daytime high-temperature periods, significantly increasing electricity expenditures. In addition, the annual operating hours of ACS have shown a continuous upward trend [1]. In response, industries have been actively investing in the research and development of energy-efficient technologies to reduce electricity consumption and mitigate energy costs. Therefore, improving the efficiency of ACS has become an urgent and indispensable issue [2,3].

In an ACS, the power consumption of chillers accounts for approximately 60% of the total energy use. Energy-saving analyses indicate that implementing appropriate control strategies and improving the Coefficient of Performance (COP) of the chiller units are among the most effective approaches to reducing the substantial power demand associated with peak loads [4]. The most common energy-saving strategies for chillers include: (1) operating the chiller at its optimal efficiency point, and (2) increasing the chilled water outlet temperature [5,6]. In general, chillers operate most efficiently at 60% to 95% of their rated cooling capacity, and the COP exhibits an approximately linear relationship with the cooling capacity [7]. The operating efficiency of a chiller depends on the combined performance of the compressor, evaporator, and condenser [8]. If a chiller's capacity becomes insufficient due to poor design or prolonged operation, operating it near full load will only increase energy consumption without improving cooling performance. In an ACS, avoiding the operation of multiple chillers at low efficiency levels can yield significant energy savings and enhance overall system performance. Therefore, implementing real-time capacity control among multiple chillers to maintain operation near their optimal efficiency points is essential for improving the overall energy efficiency of the system.

In the field of energy-saving optimization for ACS, most studies have concentrated on the economic scheduling of chillers. These studies employ a wide range of optimization algorithms, such as particle swarm optimization [9], dynamic programming [10], Hopfield neural networks [11], genetic algorithms [12,13], simulated annealing [14], differential evolution [15], cuckoo search [16], and the firefly algorithm [17]. These algorithms adjust the chillers' capacity outputs based on the required cooling load to determine load distribution and power consumption for each unit, thereby ensuring the system operates at its most energy-efficient state and minimizing electricity costs. In recent years, with the rapid development of energy-saving technologies and equipment for ACS, various energy-conservation techniques have been widely adopted [18–20]. Intelligent control strategies for ACS can dynamically regulate the cooling capacity of chillers in response to fluctuations in a building's cooling demand. This enables chillers to operate at or near their highest efficiency points, further enhancing the overall energy efficiency of the system.

In the research on capacity control for ACS, Tu et al. proposed a control model for multi-unit ACSs to ensure stable and reliable operation while achieving both high cooling performance and energy efficiency [21]. You et al. employed a load-based sequencing control strategy to coordinate the sequencing of multiple devices and introduced a deep recurrent DRQN network that effectively utilizes historical data to optimize the operating parameters of air-conditioning water systems with chiller control [22]. Lee et al. analyzed the heat transfer process of a central variable water/air flow chiller system using a thermal resistance approach and further optimized capacity matching, with a particular focus on addressing excess condensing heat—an aspect that previous studies had often oversimplified—while considering overall energy performance [23]. Xiao et al. proposed a novel performance index, the capacity utilization rate, to illustrate the impact of indoor units on system performance, and developed a performance model based on this index [24]. The proposed model was validated through field tests in real buildings to examine the operational characteristics of variable refrigerant flow systems. Moreover, the use of diverse hybrid nanolubricant composition ratios has been shown to enhance the COP of ACSs [25].

Liu et al. presented an optimal strategy for improving chiller sequencing control to achieve energy-efficient and reliable operation [26], while Hui et al. proposed an available regulation capacity model for residential air conditioners to enhance power system flexibility and resilience [27]. Ko et al. designed a test facility that determines system capacity through refrigerant-side capacity measurement, thereby reducing fuel consumption and saving energy [28]. Wang et al. developed a reinforcement learning (RL)-based control framework for optimizing the cooling operation of chiller plants to enhance building energy efficiency [29]. Despite these advancements in chiller control technologies, a gap remains in integrating real-time optimization with control feasibility. These limitations stem from the imitation of prior optimization-based and rule-based chiller control studies, as well as the absence of simple and deployable control strategies for multi-chiller systems. There is still no widely adopted method that explicitly quantifies and leverages the marginal relationship between COP and cooling capacity in real-time chiller scheduling. Consequently, existing strategies often fail to effectively respond to dynamic variations in building loads. As a result, chillers frequently operate at suboptimal efficiency points, leading to energy waste, reduced system reliability, and increased operational costs. Therefore, enhancing the efficiency of ACSs is not only a technical challenge but also an issue of economic sustainability. The novelty of using the RC ratio for real-time marginal efficiency assessment is proposed in this paper.

This paper proposes a real-time Optimal Capacity Control (OCC) strategy for chillers in an ACS equipped with Variable Water Volume (VWV) technology [30]. The proposed method introduces a fine-tuning mechanism, the Ratio of COP variation to capacity variation (RC ratio), for real-time scheduling. This mechanism enables dynamic adjustment of the operating capacity of chillers based on real-time cooling load data, ensuring that each unit operates near its optimal COP. By continuously monitoring the performance of multiple chillers, the OCC strategy dynamically determines which units should be loaded or unloaded to achieve the highest overall system efficiency while satisfying the required cooling load. To verify the effectiveness of the proposed strategy, a numerical analysis was developed using operational data from an existing ACS. Comparative simulations were performed to evaluate the OCC strategy against a TCC strategy. The results demonstrate that OCC achieves substantial energy savings across all operating conditions. It is demonstration of improved COP and energy savings across seasonal scenarios. These findings emphasize the importance of coupling between capacity and efficiency in ACS design and offer a practical framework for developing intelligent energy-saving control strategies. Furthermore, the OCC strategy significantly improves overall system efficiency and reduces energy consumption under various load conditions.

2. Description of the Problem

This paper proposes an OCC strategy that maximizes the combined COP of all chillers while satisfying all operational constraints. The OCC optimizes the overall efficiency of the ACS, thereby reducing the total power consumption of the chillers and further enhancing the system's energy efficiency.

2.1. VWV System Configuration

The ACS investigated in this study is a VWV system, commonly found in modern commercial buildings as shown in Figure 1. The ACS utilizes a primary constant/secondary variable flow chilled water system, where the flow rate of the chilled water is modulated by variable frequency drives (VFDs) on the pumps to match the real-time cooling load. The primary side of the system includes multiple chillers and constant-frequency chilled water pumps; the secondary side uses the variable-speed chilled water pumps to supply the cooling load. The VWV system uses a common pipe to balance the chilled water flow

between the chillers and the loads. In the primary side, the constant-frequency chilled water pumps delivered chilled water \dot{Q}_1 to common pipe, which flows through \dot{Q}_2 back to the primary. Each chiller is equipped with a constant-frequency chilled water pump, delivering a fixed amount of chilled water. The secondary side is delivered the \dot{Q}_3 and \dot{Q}_4 by a variable-speed chilled water pumps with variable flow rate control. The chilled water flow control includes the opening and closing of the two-way control valve, the speed control of the variable frequency secondary pump, and the bypass control valve to maintain the pressure difference between the inlet and outlet of the load side. The system is operated to maintain the supply chilled water temperature within a defined range (6–7 °C), while meeting real-time thermal loads calculated from building demand. The chillers are the primary energy consumers in the ACS, and their combined operation significantly impacts the overall system efficiency. This study focuses on optimizing the capacity control of these chillers to minimize energy consumption while satisfying the building's cooling demand.

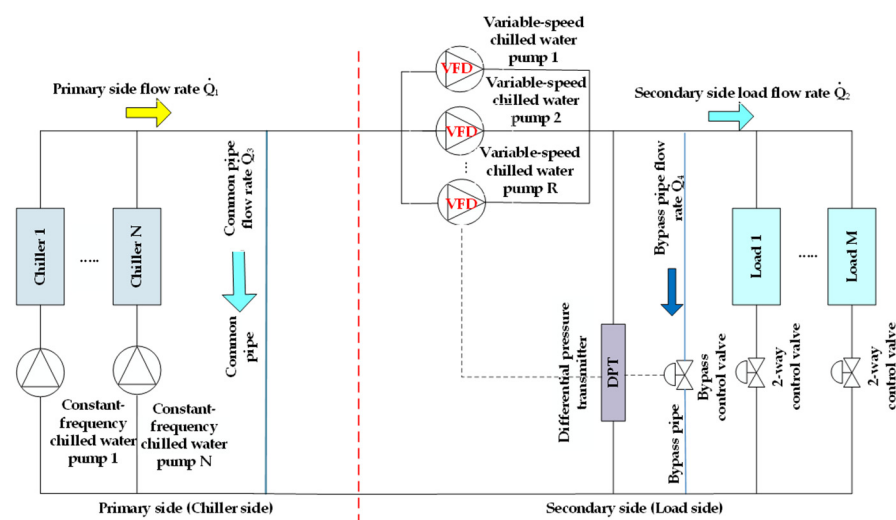


Figure 1. VVW Schematic diagram of the ACS.

2.2. The Performance Analysis of Chillers

The primary energy-saving strategy for ACSs is to precisely control the VVW system for both chilled water flow and cooling water flow, ensuring that the cooling load requirements are fully met without unnecessary energy waste. The efficiency of the chilled water unit is represented by the COP, as shown in Equation (1) [31].

$$COP_i(t) = \frac{Q_i^{cool}(t)}{P_i^{elec}(t)} \quad (1)$$

While it is often assumed that a chiller's performance is fixed after manufacturing, its COP is not a static value. In practice, the COP varies dynamically with operating conditions and often deviates from its nominal rated value. Although the relationship between COP and cooling capacity is approximately linear for both volumetric and centrifugal chillers, the overall operational efficiency depends on the integrated performance of the compressor, evaporator, and condenser. If the heat-exchange capability of the evaporator or condenser deteriorates over time—due to factors such as undersized design, fouling, or long-term operational wear—a critical issue may arise: operating the chiller near full load can increase power consumption without delivering a corresponding improvement in cooling output [32]. Consequently, the unit is forced to operate in a low-COP state, as illustrated in Figure 2.

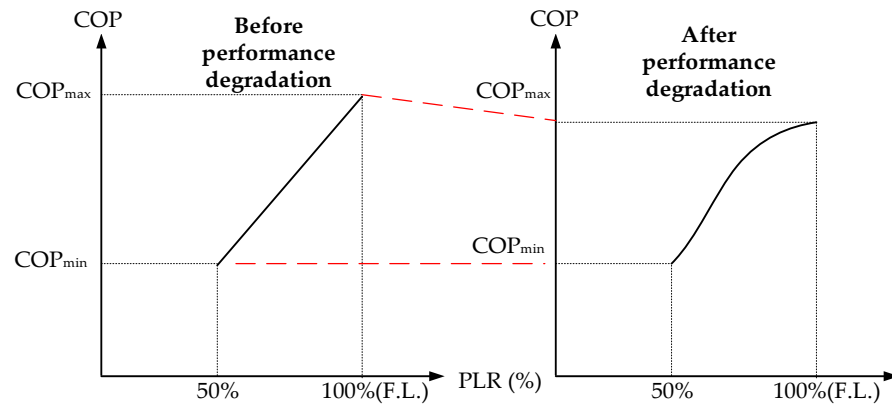


Figure 2. COP variation due to chiller degradation.

Figure 2 provides a simplified conceptual illustration of COP degradation within a typical operating range. In practice, the COP–capacity relationship is not strictly linear and varies depending on compressor type and control mechanism. The approximately linear trend observed in some chillers is generally valid only within moderate part-load regions. For purely quantity-controlled machines operating under on/off control, the COP behavior may exhibit discontinuities and cannot be represented by a linear relationship between COP_{min} and COP_{max} . Therefore, the linear depiction in Figure 2 should not be interpreted as a universal theoretical assumption but rather as an illustrative trend within a specific operating context.

2.3. The Operating Characteristic Curve of Chiller

The COP of a chiller varies according to its operating conditions. When an ACS adopts a VWV system for energy savings, the chiller’s automatic control system adjusts its cooling capacity to match fluctuations in the cooling load. However, if the operating capacity of the chiller is not properly regulated, its COP will decrease. The COP generally changes with the Part Load Ratio (PLR) of the chiller, which is defined as shown in Equation (2). The PLR is defined as the ratio between the operating cooling capacity and the rated cooling capacity of the chiller, which is a standard performance indicator widely adopted in the HVAC engineering literature [9].

$$PLR_i(t) = \frac{P_i^{cool}(t)}{P_i^{rated}} \times 100\% \quad (2)$$

The operating characteristics curves of chillers describe the relationship between the PLR and the COP. The operating characteristic curve of a chiller is typically approximated by a quadratic function [9], as shown in Equation (3).

$$COP_i(t) = a_i \cdot PLR_i^2(t) + b_i \cdot PLR_i(t) + c_i \quad (3)$$

The core of this model is to establish the relationship between a chiller’s operating capacity and its COP. Analysis of the operational data revealed a quadratic relationship between the cooling capacity and COP for each chiller. By applying polynomial regression to the collected data, performance curves were fitted for the primary chillers in the system. The ACS employs a VWV strategy to regulate the chillers’ cooling capacities in response to fluctuations in the cooling load. However, if the chiller capacity is not properly controlled, it may result in excessively high condenser pressure or excessively low evaporator pressure. Both of these conditions are detrimental to chiller performance and lead to a reduction in COP.

It should be noted that the COP–PLR relationship may vary depending on the type of chiller and compressor mechanism. These differences arise from variations in compressor design, capacity modulation mechanisms, and thermodynamic characteristics. The proposed OCC strategy does not rely on a predefined linear COP assumption. Instead, it is formulated based on empirically derived operating characteristic curves and their corresponding first-order derivatives. The RC ratio used in this study represents the marginal variation of COP with respect to cooling capacity at a specific operating point. Therefore, as long as the COP–capacity relationship of a given chiller type can be accurately modeled or monitored, the marginal equalization mechanism remains applicable.

3. Formulation of the OCC Strategy

The objective of the OCC strategy is to dynamically distribute the total cooling load among multiple chillers so as to maximize the overall COP of the system.

3.1. Problem Formulation

The optimization problem is formulated to maximize the sum of the COP of all chillers. The objective function can be expressed as follows:

$$\text{Maximize } COP_T = \sum_{i=1}^N COP_i = \sum_{i=1}^N a_i \cdot PLR_i^2 + b_i \cdot PLR_i + c_i \quad (4)$$

The relative constraints are described as follows.

1. Load satisfaction constraint: The total cooling output from all chillers must match the total cooling load of the system.

$$\sum_{i=1}^N PLR_i \cdot P_i^{rated} = P_T \quad (5)$$

2. Operational constraint: The operating capacity of each chiller must remain within its allowable minimum and maximum limits.

$$P_{i,min}^{cool} \leq P_i^{cool} \leq P_{i,max}^{cool} \quad \forall i = \{1, \dots, N\} \quad (6)$$

3.2. Traditional Capacity Control (TCC)

The formulated optimization problem is solved using the Lagrange multiplier method [33]. The Lagrangian function (\mathcal{L}) is constructed by combining the objective function with the equality constraint, as shown in Equation (7).

$$\mathcal{L}(PLR_1, \dots, PLR_N, \lambda) = COP_T + \lambda \left(P_T - \sum_{i=1}^N PLR_i \cdot P_i^{rated} \right), \quad (7)$$

For the objective function to be at its maximum, the partial derivatives of the Lagrangian function with respect to each variable (PLR_i and λ) must be equal to zero. The partial derivative of the Lagrangian function with respect to PLR_i for each chiller is given as follows:

$$\frac{\partial \mathcal{L}}{\partial PLR_i} = \frac{\partial (COP_i)}{\partial PLR_i} + \lambda \left(-P_i^{rated} \right) = 0 \quad (8)$$

Equation (8) can be rearranged as follows:

$$\frac{\partial (COP_i)}{\partial PLR_i} \cdot \frac{1}{P_i^{rated}} = \lambda \quad (9)$$

By applying the chain rule, since $P_i^{cool} = PLR_i \cdot P_i^{rated}$, the derivative of the part-load ratio can be expressed as

$$\partial PLR_i = \frac{\partial P_i^{cool}}{P_i^{rated}} \tag{10}$$

Substituting Equation (10) into Equation (9), a new equation can be expressed as

$$\frac{\partial(COP_i)}{\partial P_i^{cool}} = \lambda \tag{11}$$

Equation (11) reveals the fundamental principle of the proposed OCC strategy, λ represents the rate of change of each chiller’s COP with respect to its cooling capacity. In other words, λ quantifies how much the COP of chiller i increases (or decreases) when its cooling load is slightly adjusted.

3.3. OCC Strategy

Since the capacity and COP values vary continuously during chiller operation, recording the COP and cooling capacity of each chiller at regular intervals enables continuous determination of the RC value. The ratio of COP change to capacity change is expressed in Equation (12).

$$RC_i(t) = \frac{COP_i(t) - COP_i(t - 1)}{|P_i^{cool}(t) - P_i^{cool}(t - 1)|} = \frac{\Delta COP_i(t)}{\Delta P_i^{cool}(t)} \tag{12}$$

The RC ratio provides essential information about the chiller’s marginal performance. The fine-tuning mechanism is designed to take actions that achieve the highest possible efficiency improvement for the entire system. This control strategy operates in two primary modes: loading and unloading.

Loading Mode: When the total system cooling load increases ($P_i^{cool}(t) > P_i^{cool}(t - 1)$), a chiller must be selected to increase its cooling output. The algorithm prioritizes the chiller that provides the greatest increase in COP for a given increase in capacity.

- A positive RC ratio ($RC > 0$) during the loading process indicates that the chiller’s COP increases as its capacity increases. The COP operating curve from point A to point B is illustrated in Figure 3a.
- A negative RC ratio ($RC < 0$) indicates that the COP decreases as cooling capacity increases. The COP operating curve from point C to point D is illustrated in Figure 3b. To maximize system efficiency, the controller selects the chiller with the highest RC ratio to accommodate the additional cooling load.

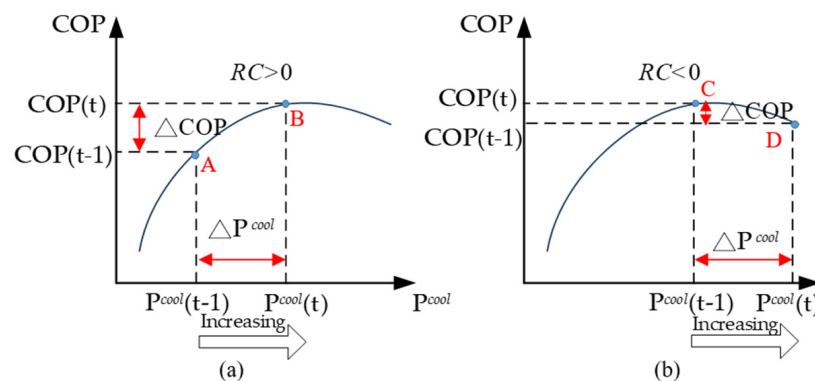


Figure 3. Illustration of COP change during the loading process.

Unloading Mode: When the total system cooling load decreases ($P_i^{cool}(t) < P_i^{cool}(t - 1)$), a chiller must be selected to reduce its cooling output. In this scenario, the objective is to

select the chiller whose reduction in cooling capacity yields the greatest improvement or smallest degradation in its COP.

- $RC < 0$ indicates that the COP value of the chiller decreases as the operating capacity adjustment decreases as shown in Figure 4a. The COP operating curve from point E to point F is illustrated in Figure 4a. $RC > 0$ indicates that the COP value of the chiller increases as the operating capacity adjustment decreases as shown in Figure 4b. The COP operating curve from point G to point H is illustrated in Figure 4b.
- To clarify, during unloading, the change in capacity is negative. A high positive RC value indicates that a small reduction in cooling load results in a substantial increase in the COP. This represents the most favorable condition for unloading. Therefore, when the system needs to shed load, the controller also selects the chiller with the highest RC ratio for unloading.

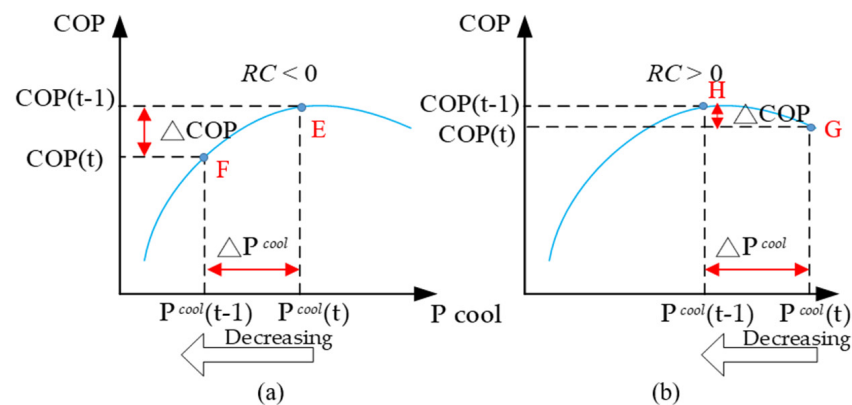


Figure 4. Illustration of COP change during the unloading process.

In summary, at any control interval t that requires an adjustment in total cooling output, the system identifies the chiller with the maximum RC ratio among all active units to perform either loading or unloading. This relationship can be formally expressed as follows:

$$RC_{max}^L(t) = \text{Max.}_{i=1,2,\dots,N} \{RC_i^L(t)\} \quad (13)$$

$$RC_{max}^U(t) = \text{Max.}_{i=1,2,\dots,N} \{RC_i^U(t)\} \quad (14)$$

This unified criterion ensures that the system continuously seeks the operating point of highest marginal efficiency, dynamically adapting to load variations to maintain optimal overall performance.

3.4. Implementation of the OCC

The principles of the fine-tuning mechanism are integrated into a comprehensive control strategy that is executed at each control interval. The overall operational flow of the OCC strategy is illustrated in the flowchart shown in Figure 5. The procedure of the fine-tuning mechanism can be summarized as follows:

1. System Initialization: The control program initializes by reading the predefined system parameters, including the number of chillers and their corresponding performance curve models.
2. Load Calculation: The system calculates the real-time total cooling load, P_T , based on sensor data collected from the building.

3. Capacity Evaluation: The current total online capacity, P_T^{cool} , is determined by summing the outputs of all active chillers. This value is then compared with the required load, P_T .
4. Load Distribution (Modulation):
 - (a) The system computes the RC ratio for each online chiller based on its current and previous operational data.
 - (b) The chiller with the maximum RC ratio is identified.
 - (c) The selected chiller then adjusts its cooling capacity—either loading or unloading—to align the total online capacity with the required system load.
5. Chiller Staging (Startup/Shutdown): After the load distribution, the system evaluates the operating state of all chillers. If the total load exceeds the combined capacity of the online units, a standby chiller is activated. Conversely, if a chiller operates below its minimum load threshold for a sustained period, it is shut down to avoid inefficient operation.
6. Loop: The system waits for the next control time step and repeats the entire process from Step 2, thereby ensuring continuous and dynamic optimization of the unit's overall performance.

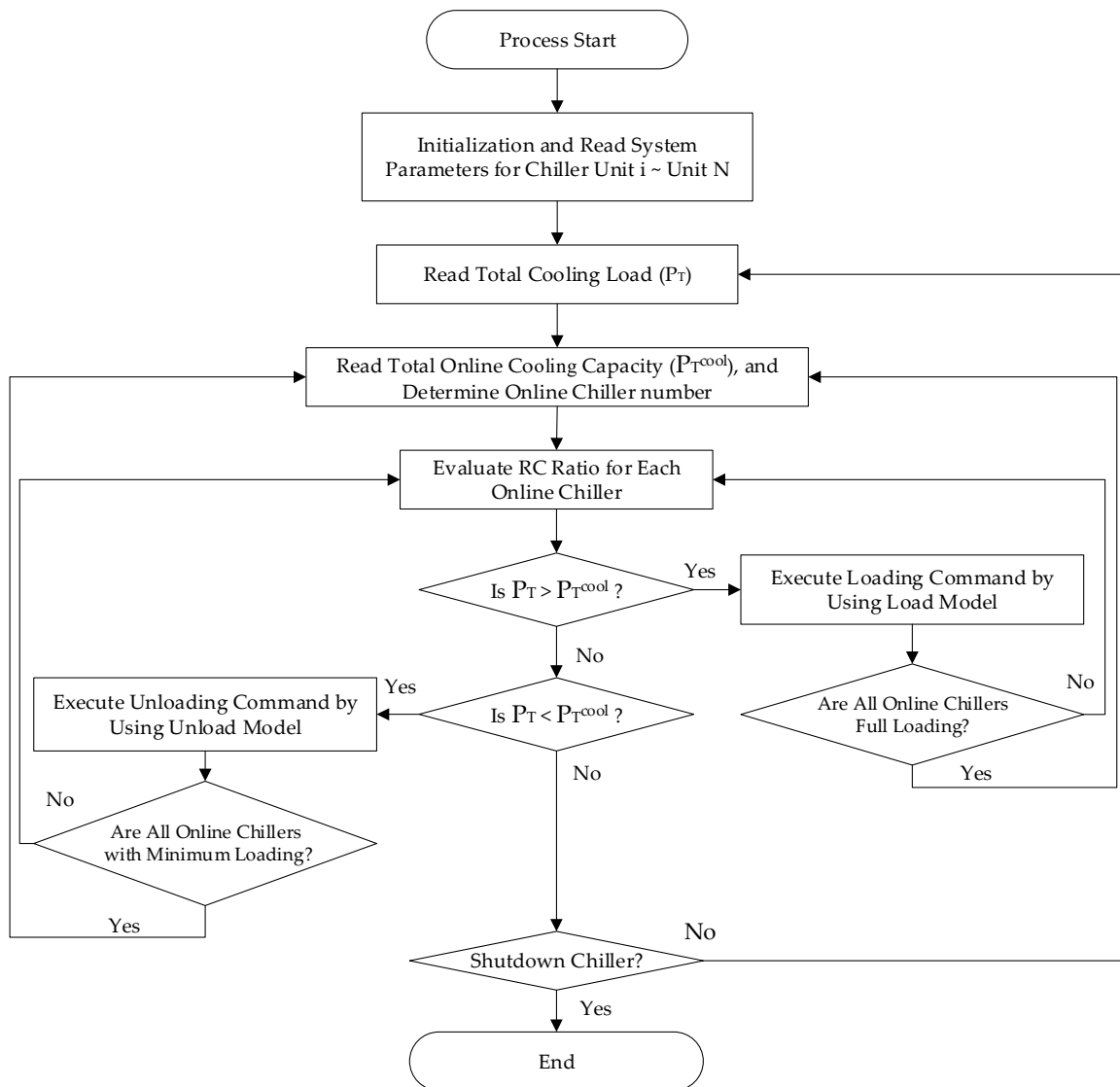


Figure 5. Flow Chart of the OCC process.

4. Case Study

This study uses an office building as the test case. The analysis focuses on a single representative day from a typical summer week. Three chiller units, KLSB-01, KLSB-02, and KLSB-03, are employed in the test. The corresponding cooling load and electricity price during summer are presented in Table 1. Table 2 shows the specification of the ACS. The numerical computations were performed using MATLAB R2018b on a PIV-2.6GHZ computer with 512MB RAM. The optimization procedures, RC ratio calculation, load redistribution logic, and seasonal energy consumption analysis were implemented through custom-developed scripts. The simulation model was constructed based on actual operational data collected from the ACS of the studied office building. The monitored dataset includes cooling capacity, electrical power consumption, chilled water temperature, and part-load ratio (PLR) under stable operating conditions. Polynomial regression was applied to derive the COP–PLR characteristic curves for each chiller. These fitted curves serve as the performance model for simulation.

Table 1. Cooling load and electricity price during summer.

Time Section	Electricity Price (NTD \$/kWh)	Cooling Load (RT)
08–09	2.18	214.6
09–10	5.02	178.8
10–11	5.02	178.8
11–12	5.02	178.8
12–13	5.02	214.6
13–14	5.02	214.6
14–15	5.02	178.8
15–16	5.02	178.8
16–17	8.05	143.0
17–18	8.05	107.3

Table 2. Specification of the ACS.

No.	Item	Specification
1	Model	KLSB-100S
2	Power Source	3 ϕ 380V 60 Hz
3	Refrigerant	R134a
4	Air conditioning capability	300 kW
5	Power consumption (air conditioner)	60 kW
6	COP (Full air conditioning)	5.0

4.1. Implement of RC Ratio

This study employs a monitoring system to record the COP values corresponding to chiller capacity adjustments from 10% to 100% of the PLR, as shown in Table 3. The measurement environment was at an outdoor temperature of 35 °C and an indoor temperature of 28 °C. Data are obtained directly from the existing monitoring system of the building's ACS. The ACS is equipped with a commercial-grade control and monitoring system capable of continuously measuring chilled-water temperatures, flow rates, cooling capacities, condenser-side parameters, and the power consumption of each chiller. Based on these recorded data, a curve-fitting method was applied to derive the operating characteristic curve of the chillers.

Table 3. The relationship between COP and PLR.

PLR (%)	The COP of Chillers		
	KLSB-01	KLSB-02	KLSB-03
100	4.97	4.91	4.98
96	4.96	4.87	4.96
95	4.95	4.85	4.94
90	4.92	4.82	4.91
87	4.91	4.80	4.87
85	4.90	4.75	4.84
83	4.83	4.73	4.83
80	4.82	4.70	4.80
77	4.81	4.56	4.80
75	4.70	4.50	4.75
72	4.66	4.47	4.69
70	4.55	4.42	4.60
67	4.35	4.42	4.55
65	4.15	4.40	4.25
62	4.11	4.23	4.18
60	3.85	4.15	3.95
57	3.77	3.93	3.77
55	3.75	3.85	3.65
50	3.65	3.80	3.55
45	3.65	3.75	3.45
42	3.6	3.66	3.39
40	3.55	3.61	3.34
37	3.46	3.54	3.34
35	3.35	3.45	3.29
32	3.24	3.39	3.22
30	3.15	3.33	3.11
27	3.03	3.33	3.06
25	2.86	3.11	2.86
20	2.75	2.93	2.79
18	2.67	2.77	2.70
16	2.53	2.65	2.63
14	2.35	2.53	2.55
12	2.24	2.45	2.44
10	2.15	2.34	2.36

By applying curve fitting method, the operating characteristic curves of chillers for units KLSB-01, KLSB-02, and KLSB-03 are derived as shown in Equations (15)–(17).

$$COP_1 = -0.000193PLR_1^2 + 0.0476PLR_1 + 1.6893 \tag{15}$$

$$COP_2 = -0.000193PLR_2^2 + 0.0472PLR_2 + 1.8847 \tag{16}$$

$$COP_3 = -0.0002PLR_3^2 + 0.0489PLR_3 + 1.9531 \tag{17}$$

By taking the first differential of the capacity–COP relationship, the corresponding first-derivative trend curves COP'_1 , COP'_2 , and COP'_3 are obtained as shown in Equations (18)–(20).

$$COP'_1 = -0.000386PLR_1 + 0.0476 \tag{18}$$

$$COP'_2 = -0.000386PLR_2 + 0.0472 \tag{19}$$

$$COP'_3 = -0.00040PLR_3 + 0.0493 \tag{20}$$

Figure 6 presents the relationship between the RC value and the operating capacity of each chiller under the OCC strategy. In this figure, the horizontal axis represents the RC value, defined as the marginal variation of COP with respect to cooling capacity. The left vertical axis indicates the individual operating capacity of each chiller, while the right vertical axis represents the total combined capacity of the three chillers. In this case, the system cooling load is 214.6 RT. The OCC strategy adjusted the chiller capacities based on their respective RC values. The procedure for the fine-tuning mechanism based on RC values is summarized as follows:

1. The RC value corresponds to the first-order derivative of the COP–capacity relationship derived from Equations (18)–(20), and it reflects the marginal efficiency improvement per unit of capacity adjustment. According to the optimality condition derived from the Lagrangian formulation in Section 3, the optimal operating point is achieved when the marginal COP variation of all operating chillers becomes equal. Therefore, the OCC strategy sequentially adjusts chiller capacities by always selecting the unit with the highest RC value.
2. At the initial stage, all chillers operate at their minimum allowable capacity. Among them, KLSB-03 exhibits the highest RC value (approximately 0.045) at 10% loading, indicating that increasing its capacity will yield the greatest COP improvement per unit of load increase. Therefore, KLSB-03 is selected first for loading, as shown at Point A in Figure 6. As its capacity increases toward approximately 25% (Point B), its RC value gradually decreases due to the downward trend of the derivative curve.
3. Once the RC value of KLSB-03 decreases to a level comparable to the other chillers, the controller evaluates the RC values of all units again. The chiller with the highest current RC value is then selected for further loading. This iterative process continues such that the operating points of the chillers gradually converge toward a state where their RC values are approximately equal (around 0.039 in this case). At this stage, the marginal efficiency contributions of all operating chillers are balanced, indicating that the system has reached a locally optimal capacity distribution.
4. The loading sequence is repeated until the total combined cooling capacity matches the required system load of 214.6 RT. This marginal equalization mechanism ensures that each incremental increase in load is assigned to the chiller that provides the highest efficiency gain, thereby maximizing the overall system COP.
5. During unloading, the same marginal principle applies. Because capacity reduction implies a negative change in cooling output, the RC value is evaluated accordingly, and the chiller with the highest RC value (i.e., yielding the greatest efficiency improvement per unit of capacity reduction) is selected for unloading. This unified marginal-efficiency criterion guarantees that the system continuously operates at the most energy-efficient configuration under both increasing and decreasing load conditions.

Because the cooling capacity and COP vary simultaneously, optimizing one without accounting for the other may result in operational inefficiency. By calculating the RC values of all chillers in operation, the control system can identify the unit that provides the greatest efficiency gain per unit of capacity adjustment. This approach ensures that the system's overall COP is maximized while fully satisfying the cooling load demand.

4.2. Daily OCC Strategy in Summer

The capacity control of each chiller was performed using both the TCC and the OCC strategies. The daily capacity allocation results are presented in Tables 4 and 5. Under the TCC strategy, as shown in Table 4, the capacity of KLSB-03 was set to a minimum of 50%, while the remaining cooling load was evenly distributed between KLSB-01 and KLSB-02.

This approach represents the optimal configuration for traditional chiller capacity control under low-efficiency operating constraints. Consequently, units KLSB-01 and KLSB-02 were forced to operate at higher COP levels, providing a suitable benchmark for comparison with the OCC strategy’s performance.

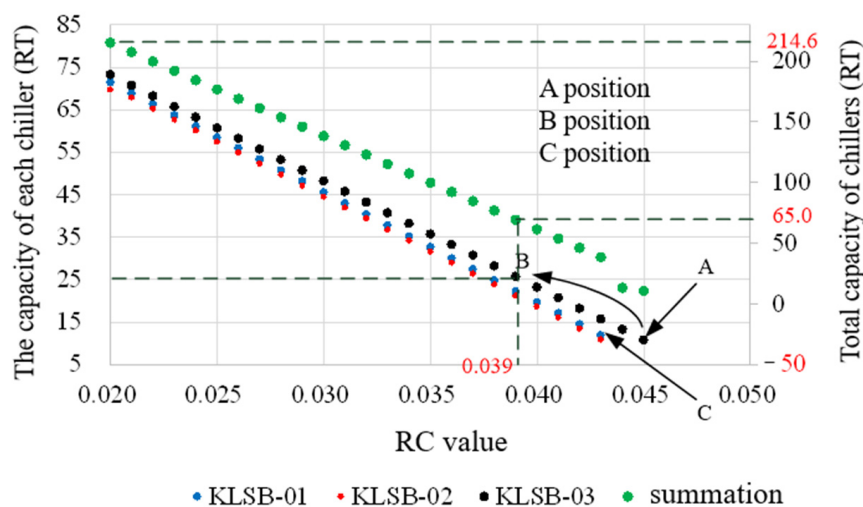


Figure 6. Relationship between RC value and chiller capacity output under the OCC.

Table 4. Daily load distribution of the TCC strategy in summer.

Time Section	Allocated Capacity (RT)			Total Load (RT)
	KLSB-01	KLSB-02	KLSB-03	
08–09	82.3	82.3	50.0	214.6
09–10	64.4	64.4	50.0	178.8
10–11	64.4	64.4	50.0	178.8
11–12	64.4	64.4	50.0	178.8
12–13	82.3	82.3	50.0	214.6
13–14	82.3	82.3	50.0	214.6
14–15	64.4	64.4	50.0	178.8
15–16	64.4	64.4	50.0	178.8
16–17	93.0	50.0	0.0	143.0
17–18	57.3	50.0	0.0	107.3

Table 5. Daily load distribution of the OCC strategy in summer.

Time Section	Allocated Capacity (RT)			Total Load (RT)
	KLSB-01	KLSB-02	KLSB-03	
08–09	71.5	69.8	73.3	214.6
09–10	61.1	54.4	63.3	178.8
10–11	58.5	57.5	60.8	178.8
11–12	58.5	57.5	60.8	178.8
12–13	71.5	69.8	73.3	214.6
13–14	71.5	69.8	73.3	214.6
14–15	61.1	54.4	63.3	178.8
15–16	61.1	54.4	63.3	178.8
16–17	69.8	0.0	73.3	143.0
17–18	51.6	0.0	55.8	107.3

A comparison in Table 5 shows that the capacity of KLSB-03 under the OCC is consistently higher than that of the other chillers. The variation in KLSB-03’s operating capacity is

also greater than that of the other units at every operating point. Consequently, whenever the ACS load increases, KLSB-03 is prioritized for capacity adjustment. After KLSB-03's capacity increases, its RC value becomes lower than those of the other two chillers. At the same operating capacity, KLSB-01 exhibits a higher RC value than KLSB-02; therefore, KLSB-01 and KLSB-02 are loaded sequentially in that order. KLSB-01's RC value will then reach the maximum among the three chillers, and this cycle continues until the combined operating capacity of all chillers satisfies the ACS load.

Tables 6 and 7 present the daily COP values and daily power consumption in summer. The total COP achieved under the OCC strategy is higher than that of the TCC strategy, while the total power consumption with OCC is slightly lower. The TCC strategy uses the Lagrange multiplier method to solve this problem, which yields a solution close to a local optimum. OCC utilizes RC fine-tuning technology to further search the optimal operating point. However, the difference between the two strategies is not substantial because the TCC strategy was already optimized, with KLSB-01 and KLSB-02 operating at higher COP levels. The cooling load of the chillers in the ACS fluctuates continuously due to the VVV regulation rate. Therefore, the chiller capacities must be continuously adjusted to match these fluctuations. The OCC strategy ensures that all chillers in the system operate at high efficiency at all times, thereby avoiding excessive energy consumption within the ACS.

Table 6. Daily COP and energy consumption using TCC strategy in summer.

Time Section	KLSB-01		KLSB-02		KLSB-03		Total COP	Total Consumption
	COP	kWh	COP	kWh	COP	kWh	COP	kWh
08–09	4.3	67.0	4.5	64.5	3.9	45.1	12.7	176.6
09–10	4.0	57.1	4.1	54.7	3.9	45.1	12.0	156.9
10–11	4.0	57.1	4.1	54.7	3.9	45.1	12.0	156.9
11–12	4.0	57.1	4.1	54.7	3.9	45.1	12.0	156.9
12–13	4.3	67.0	4.5	64.5	3.9	45.1	12.7	176.6
13–14	4.3	67.0	4.5	64.5	3.9	45.1	12.7	176.6
14–15	4.0	57.1	4.1	54.7	3.9	45.1	12.0	156.9
15–16	4.0	57.1	4.1	54.7	3.9	45.1	12.0	156.9
16–17	4.5	73.1	3.7	46.6	0.0	0.0	8.2	119.8
17–18	3.8	53.1	3.8	46.6	0.0	0.0	7.6	99.7
			Total				113.9	1534.0

Table 7. Daily COP and energy consumption using OCC strategy in summer.

Time Section	KLSB-01		KLSB-02		KLSB-03		Total COP	Total Consumption
	COP	kWh	COP	kWh	COP	kWh	COP	kWh
08–09	4.1	61.0	4.2	57.7	4.5	57.7	12.8	176.4
09–10	3.9	55.3	3.9	49.2	4.2	52.4	12.0	156.8
10–11	3.8	53.8	4.0	50.9	4.2	51.0	12.0	155.8
11–12	3.8	53.8	4.0	50.9	4.2	51.0	12.0	155.8
12–13	4.1	61.0	4.2	57.7	4.5	57.7	12.8	176.4
13–14	4.1	61.0	4.2	57.7	4.5	57.7	12.8	176.4
14–15	3.9	55.3	3.9	49.2	4.2	52.4	12.0	156.8
15–16	3.9	55.3	3.9	49.2	4.2	52.4	12.0	156.8
16–17	4.1	60.0	0.0	0.0	4.4	57.7	8.5	117.8
17–18	3.6	49.8	0.0	0.0	4.1	48.3	7.7	98.1
			Total				114.8	1527.2

The OCC strategy was applied under the same load conditions, and the results were compared with those of the TCC strategy. The analysis demonstrates that:

- OCC strategy remains applicable in heterogeneous configurations.
- Load redistribution becomes more differentiated, with high-efficiency units prioritized under marginal equalization principles.
- The performance improvement over TCC is more pronounced in heterogeneous systems due to increased variability in marginal efficiency.

- Certain operational constraints may introduce staging discontinuities.

4.3. Energy Consumption Across Four Seasons

The seasonal analysis is based on monitored operational data from representative weeks in each season. The selected periods and corresponding outdoor temperature characteristics are as follows:

- Spring: April 8–12; average outdoor temperature 23–27 °C; peak daytime temperature approximately 29 °C.
- Summer: July 10–14; average outdoor temperature 30–34 °C; peak daytime temperature approximately 35–36 °C.
- Autumn: October 16–20; average outdoor temperature 24–29 °C; peak daytime temperature approximately 31 °C.
- Winter: December 4–8; average outdoor temperature 18–23 °C; peak daytime temperature approximately 25 °C.

The selected weeks represent typical climatic conditions in southern Taiwan and reflect actual cooling demand observed in the building. The energy consumption and electricity price for each season are illustrated in Figures 7 and 8. Figure 7 compares the energy consumption of the TCC and OCC strategies across the four seasons. The results show that OCC consistently achieves lower energy consumption than TCC, particularly during summer and autumn when cooling loads are high. This improvement demonstrates OCC's ability to maintain high operating efficiency by dynamically adjusting chiller capacities in response to varying load conditions. Similarly, Figure 8 compares the seasonal electricity costs under both strategies. OCC achieves lower total electricity expenditure compared to TCC throughout the year, confirming its effectiveness in reducing operating costs while maintaining sufficient cooling performance. Although the energy savings during spring and winter are less pronounced due to lighter cooling loads, OCC still provides a more balanced and adaptive response to load fluctuations. Overall, these results indicate that the OCC strategy not only enhances system efficiency but also contributes to long-term economic and energy-saving benefits across varying climatic conditions.

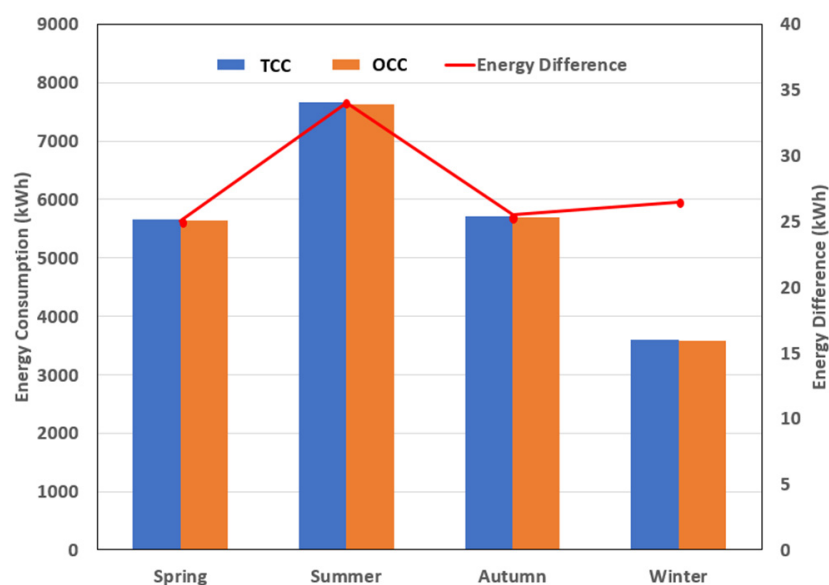


Figure 7. The comparison of energy consumption of TCC and OCC.

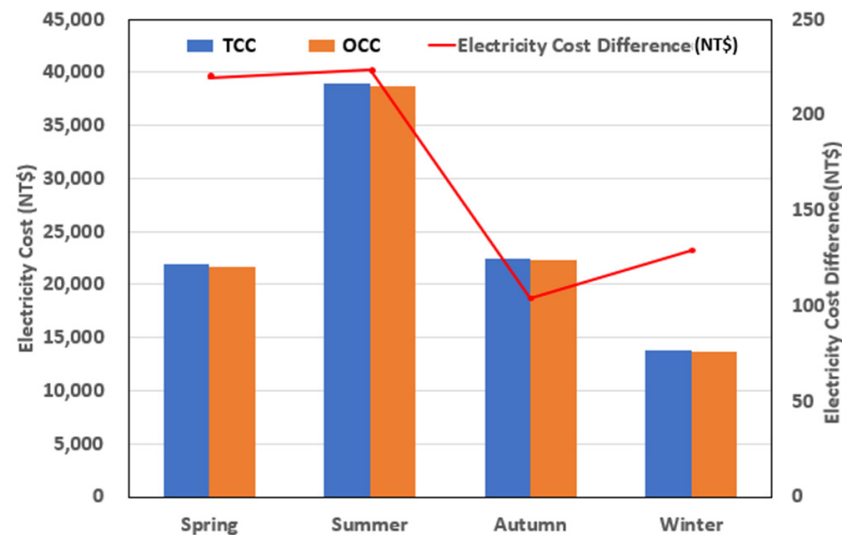


Figure 8. The comparison of electricity prices of TCC and OCC.

4.4. Applicable Scenarios and Practical Limitations of the OCC Strategy

The proposed OCC strategy is primarily designed for centralized multi-chiller air-conditioning systems, such as chiller plants in large commercial buildings, hospitals, campuses, industrial facilities, and district cooling systems. In such systems, multiple chillers operate in parallel, and load redistribution among units is feasible. The RC-based marginal equalization mechanism can dynamically determine loading and unloading priorities, thereby improving overall plant efficiency.

However, in small-scale air-conditioning systems equipped with only a single chiller, the OCC strategy cannot be directly applied. Since load redistribution among multiple units is not possible, the marginal equalization principle becomes inapplicable. In such cases, system optimization should instead focus on enhancing the part-load performance of the individual chiller, improving chilled water temperature control, or optimizing variable-speed pump operation.

For buildings with two chillers operating under simplified staging logic, partial implementation of the RC-based marginal principle may still be feasible. The strategy could be adapted to assist in startup/shutdown sequencing decisions or to support fine-tuning around medium-load operating ranges.

Future research may explore simplified OCC variants tailored for small-scale systems, such as:

- Integrating marginal COP estimation into single-chiller part-load optimization.
- Combining the RC concept with predictive load forecasting.
- Developing hybrid control strategies that coordinate chiller operation with auxiliary components.

By clarifying the applicable deployment context, the OCC strategy should be understood as a plant-level optimization framework rather than a universal solution for all air-conditioning configurations.

5. Conclusions

This study aims to develop an OCC strategy for chillers in ACS. The proposed method uses a fine-tuning mechanism to dynamically adjust the operating capacity of the chillers according to the real-time cooling load, ensuring that each unit operates near its optimal efficiency point. This strategy enables a precise match between chiller capacity and cooling load, thereby maximizing system efficiency while reducing both energy consumption and

operating costs. The OCC strategy employs the RC ratio algorithm to determine loading and unloading actions by calculating the ratio between the changes in the COP and cooling capacity for each chiller. To verify the effectiveness of the proposed strategy, numerical simulations were conducted to compare the OCC and TCC strategies. The analytical results confirm the validity of the proposed optimization method.

During a typical summer day, the total power consumption under the OCC strategy was 1527.2 kWh, slightly lower than the 1534.0 kWh consumed under TCC. Furthermore, the system COP increased from 113.9 (TCC) to 114.8 (OCC), highlighting the OCC strategy's superior performance even under peak load conditions. This study integrates theoretical optimization, empirical data modeling, numerical simulation, and control strategy design, all grounded in established engineering methodologies. It not only demonstrates the real-time control mechanism but also aligns with the principles of feedback-based adaptive control systems in engineering.

Future research may focus on large-scale validation, integration with predictive or model-based control strategies, and incorporation of dynamic electricity pricing into the objective function. Hybrid approaches combining marginal-efficiency control with advanced optimization or learning-based algorithms may further enhance robustness and global optimality. Overall, the proposed OCC strategy provides a practical and physically interpretable framework for improving chiller plant efficiency. By explicitly leveraging the marginal relationship between capacity and COP, the method bridges theoretical optimization principles and real-time operational control, offering a scalable solution for energy-efficient air-conditioning system management.

Author Contributions: Conceptualization, M.-T.T.; Methodology, T.-S.Z.; Software, T.-S.Z.; Validation, K.-W.C.; Formal analysis, T.-S.Z.; Investigation, K.-W.C.; Resources, K.-W.C.; Data curation, K.-W.C.; Writing—review and editing, M.-T.T.; Visualization, M.-T.T.; Supervision, M.-T.T.; Project administration, M.-T.T. All authors have read and agreed to the published version of the manuscript.

Funding: This research was funded by Ministry of Science and Technology, Taiwan (Grant Nos. NSTC 114-2637-E-230-003).

Data Availability Statement: The original contributions presented in this study are included in the article. Further inquiries can be directed to the corresponding author.

Conflicts of Interest: The authors declare no conflicts of interest.

Abbreviations

The following abbreviations are used in this manuscript:

ACS	air-conditioning system
AHU	Air-Handling Unit
COP	Coefficient of Performance
OCC	Optimal Capacity Control
PLR	Part Load Ratio
RL	Reinforcement Learning
TCC	Traditional Capacity Control
VFD	variable frequency drives
VPF	Variable primary flow
VWV	Variable Water Volume
P_i	Electrical input power of chiller i
$P_{i,max}^{cool}$	The maximum operational capacities of the i -th chiller
$P_{i,min}^{cool}$	The minimum operational capacities of the i -th chiller
P_i^{rated}	The rated cooling capacity of the i -th chiller.
P_T	The total system cooling load

\dot{Q}_i	Cooling capacity of chiller i
$\dot{Q}_{rate,i}$	Rated cooling capacity of chiller i
COP_T	the objective function
$COP_i(t)$	COP of chiller i at time t .
$COP_i(t-1)$	COP of chiller i from the previous time interval $t-1$
PLR_i	Part-load ratio of chiller i
$P_i^{elec}(t)$	The electrical power consumed by chiller i at time t
$Q_i^{cool}(t)$	The cooling capacity provided by chiller i at time t
$Q_i^{cool}(t-1)$	The cooling capacity provided from the previous time interval $t-1$
$RC_i(t)$	The RC ratio for the i -th chiller at time interval t
$RC_i^L(t)$	The loading RC value of the chills i at the period t
$RC_i^U(t)$	The unloading RC value of the chills i at the period t
L	Total system cooling load
N	Number of online chillers
λ	Lagrange multiplier
a_i, b_i, c_i	Polynomial coefficients of COP–PLR curve
t	Time index

References

- Energy Administration, Ministry of Economic Affairs. 2022 Annual Report on Energy Audit for Non-Production Industries. December 2022. Available online: https://ea01.moeaea.gov.tw/e0406/01/Knowledge/knowledge_more?id=62a1b665024e48bbaee45648565110f0 (accessed on 1 March 2025).
- Hussein, N.A.; Jubori, A.; Abdul-Zahra, A. Enhancing the performance of air conditioning systems by integrating phase change materials: A comprehensive review. *J. Energy Storage* **2024**, *101*, 113857. [\[CrossRef\]](#)
- Lin, W.M.; Tu, C.H.; Tsai, M.T.; Lo, C.C. Optimal Energy Reduction Schedules for Ice Storage Air-Conditioning Systems. *Energies* **2015**, *8*, 10504–10521. [\[CrossRef\]](#)
- Pieper, H.; Krupenski, I.; Brix, W.; Siirde, A.; Volkova, A. Method of linear approximation of COP for heat pumps and chillers based on thermodynamic modelling and off-design operation. *Energy* **2021**, *230*, 120743. [\[CrossRef\]](#)
- Chua, K.J.; Chou, S.K.; Yang, W.M.; Yan, J. Achieving better energy-efficient air conditioning—A review of technologies and strategies. *Appl. Energy* **2013**, *104*, 87–104. [\[CrossRef\]](#)
- Chang, Y.C.; Lin, F.A.; Lin, C.H. Optimal chiller sequencing by branch and bound method for saving energy. *Energy Convers. Manag.* **2005**, *46*, 2158–2172. [\[CrossRef\]](#)
- Cheng, Y.H.; Shih, C. Maximizing the cooling capacity and COP of two-stage thermoelectric coolers through genetic algorithm. *Appl. Therm. Eng.* **2006**, *26*, 937–947. [\[CrossRef\]](#)
- Wang, Y.; Yu, J.; Wang, Z.; Liu, G. Improved nutcracker optimization algorithm for energy-saving optimization in chiller plants: An industrial building case study. *J. Build. Eng.* **2025**, *110*, 113084. [\[CrossRef\]](#)
- Lee, W.S.; Lin, L.C. Optimal chiller loading by particle swarm algorithm for reducing energy consumption. *Appl. Therm. Eng.* **2009**, *29*, 1730–1734. [\[CrossRef\]](#)
- Chang, Y.C. An outstanding method for saving energy of optimal chiller operation. *IEEE Trans. Energy Convers.* **2006**, *21*, 527–532. [\[CrossRef\]](#)
- Chang, Y.C.; Chen, W.H. Optimal chilled water temperature calculation of multiple chiller systems using Hopfield neural network for saving energy. *Energy* **2009**, *34*, 448–456. [\[CrossRef\]](#)
- Chang, Y.C. Genetic algorithm based optimal chiller loading for energy conservation. *Appl. Therm. Eng.* **2005**, *25*, 2800–2815. [\[CrossRef\]](#)
- Chang, Y.C. Optimal chiller loading by genetic algorithm for reducing energy consumption. *Energy Build.* **2005**, *37*, 147–155. [\[CrossRef\]](#)
- Chang, Y.C.; Chen, W.H.; Lee, C.Y.; Huang, C.N. Simulated annealing based optimal chiller loading for saving energy. *Energy Convers. Manag.* **2006**, *47*, 2044–2058. [\[CrossRef\]](#)
- Lee, W.S.; Chen, Y.T.; Kuo, Y. Optimal chiller loading by differential evolution algorithm for reducing energy consumption. *Energy Build.* **2011**, *43*, 599–604. [\[CrossRef\]](#)
- Coelho, S.L.D.; Klein, C.E.; Sabat, S.L.; Mariani, V.C. Optimal chiller loading for energy conservation using a new differential cuckoo search approach. *Energy* **2014**, *75*, 237–243. [\[CrossRef\]](#)
- Coelho, S.L.D.; Mariani, V.C. Improved firefly algorithm approach applied to chiller loading for energy conservation. *Energy Build.* **2013**, *59*, 273–278. [\[CrossRef\]](#)

18. Yu, F.W.; Chan, K.T. Improved energy performance of air cooled centrifugal chillers with variable chilled water flow. *Energy Convers. Manag.* **2008**, *49*, 1595–1611. [[CrossRef](#)]
19. Li, B.; Yong, J.; Yu, L.; Yang, X.; Zhang, X.; Muhieldeen, M. A review of research on intelligent technology in building air conditioning system optimization. *Int. J. Refrig.* **2025**, *176*, 205–225. [[CrossRef](#)]
20. Mendes, R.d.P.; Garcia Pábon, J.J.; Ferreira Pottie, D.L.; Machado, L. Artificial intelligence strategies applied in general and automotive air conditioning control: A review of the last 20 years. *Int. J. Refrig.* **2024**, *164*, 180–198. [[CrossRef](#)]
21. Tu, Q.; Zou, D.; Deng, C.; Zhang, J.; Hou, L.; Yang, M.; Nong, G.; Feng, Y. Investigation on output capacity control strategy of variable refrigerant flow air conditioning system with multi-compressor. *Appl. Therm. Eng.* **2016**, *99*, 280–290. [[CrossRef](#)]
22. You, Y.; Yuan, W.; Yang, B.; Guo, C.; Zhang, K. DRQN-based global optimal control of air conditioning water system. *Energy Build.* **2024**, *323*, 114845. [[CrossRef](#)]
23. Lee, J.H.; Cheon, S.U.; Jeong, W. Multi-objective optimization for capacity matching and energy performance of heat-pump-driven liquid-desiccant air-conditioning system. *Appl. Therm. Eng.* **2023**, *119*, 120615. [[CrossRef](#)]
24. Xiao, H.; Liu, S.; Ding, Y.; Zheng, C.; Luo, B.; Niu, H.; Shi, J.; Wang, B.; Song, Q.; Shi, Q. Operation characteristics based on a novel performance model based on capacity utilization rate of a variable refrigerant flow air conditioning system. *Energy Build.* **2023**, *294*, 113253. [[CrossRef](#)]
25. Zawawi, N.; Azmi, W.; Ghazali, M.; Ali, H. Performance of Air-Conditioning System with Different Nanoparticle Composition Ratio of Hybrid Nanolubricant. *Micromachines* **2022**, *13*, 1871. [[CrossRef](#)] [[PubMed](#)]
26. Liu, Z.; Tang, H.; Luo, D.; Yu, G.; Li, J.; Li, Z. Optimal chiller sequencing control in an office building considering the variation of chiller maximum cooling capacity. *Energy Build.* **2017**, *140*, 430–442. [[CrossRef](#)]
27. Hui, H.; Yu, P.; Zhang, H.; Dai, N.; Jiang, W.; Song, Y. Regulation capacity evaluation of large-scale residential air conditioners for improving flexibility of urban power systems. *Int. J. Electr. Power Energy Syst.* **2022**, *142*, 108269. [[CrossRef](#)]
28. Ko, G.S.; Raza, W.; Park, Y.C. Capacity control of a vehicle air-conditioning system using pulse width modulated duty cycle compressor. *Case Stud. Therm. Eng.* **2021**, *26*, 100986. [[CrossRef](#)]
29. Wang, X.; Xu, H.; Fan, C.; Tan, S.; Kang, X.; Shi, Y.; Yan, D. Leveraging reinforcement learning for optimal control of chiller plant with complex hydraulic and thermodynamic characteristics. *Energy Build.* **2025**, *344*, 116037. [[CrossRef](#)]
30. Lin, Y.; Wang, H.; Hu, P.; Yang, W.; Hu, Q.; Zhu, N.; Lei, F. A study on the optimal air, load and source side temperature combination for a variable air and water volume ground source heat pump system. *Appl. Therm. Eng.* **2020**, *178*, 115595. [[CrossRef](#)]
31. Wang, S.K. *Handbook of Air Conditioning and Refrigeration*, 2nd ed.; McGraw-Hill: New York, NY, USA, 2000.
32. Yu, F.W.; Chan, K.T. Part load performance of air-cooled centrifugal chillers with variable speed condenser fan control. *Build. Environ.* **2007**, *42*, 3816–3829. [[CrossRef](#)]
33. Haeser, G.; Ramos, A. On constraint qualifications for second-order optimality conditions depending on a single Lagrange multiplier. *Oper. Res. Lett.* **2021**, *49*, 883–889. [[CrossRef](#)]

Disclaimer/Publisher’s Note: The statements, opinions and data contained in all publications are solely those of the individual author(s) and contributor(s) and not of MDPI and/or the editor(s). MDPI and/or the editor(s) disclaim responsibility for any injury to people or property resulting from any ideas, methods, instructions or products referred to in the content.